GEOPHYSICAL RESEARCH LETTERS, VOL. 28, NO. 18, PAGES 3581-3584, SEPTEMBER 15, 2001

Interferometric and dual beam observations of daytime spread-F-like irregularities over Jicamarca

Jorge L. Chau[1] and Ronald F. Woodman

Radio Observatorio de Jicamarca, Instituto Geofísico del Perú, Lima

Abstract. We report new observations made on April 11 2000 over Jicamarca of daytime spread-F-like irregularities. These irregularities are extremely rare and were first reported by *Woodman et al.* [1985]. The main features of these new observations, which are similar to the previous ones, are that they were: (1) two orders of magnitude stronger than the incoherent scatter echoes at the F peak, (2) observed between 1400 and 1600 LT; (3) characterized by small Doppler shifts ($|v_d| < 1$ m s^{-1}); and (4) characterized by long correlation times, i.e., narrow spectral widths. The latter is interpreted as evidence that these irregularities are field aligned (very aspect sensitive in the north-south direction). On this occasion the irregularities occurred at higher altitudes than before, between 950 and 1450 km compared to 600-1000 km. The echoes in these recent observations were quite localized in the east-west direction (they were much stronger in the west beam than in the east beam). Furthermore, using interferometry we determined that the irregularities were in the form of blobs, aspect sensitive in the east-west (as well as north-south) direction with aspect angle widths as small as 0.2 degrees, particularly when the echoes were strong.

1. Introduction

In this letter, we report radar observations of daytime equatorial field-aligned irregularities (FAI) from the topside of the ionosphere. These irregularities are very uncommon, they have been observed only three times in the past, all of them over the Jicamarca Radio Observatory. *Woodman et al.* [1985] reported two events (March 26 1974 and February 1 1984), and there is a third unpublished event (only a photograph from the oscilloscope) that was observed on April 21 1982 between 1530 and 1600 LT.

These new radar observations were made on April 11 2000 as part of the April-2000 Incoherent scatter world day campaign. What is new for this time is that the Jicamarca radar was operating in the new east-west dual beam interferometer mode used for zonal and vertical drift measurements [*Kudeki et al.*, 1999], which allows us to extract more information on the daytime irregularities compared to the previous observations.

As before, we are referring to these new observations as daytime equatorial spread F (ESF) irregularities for consistency. However, we think the name is questionable since these events were not observed with the Jicamarca ionosonde. ESF irregularities are common nighttime phenomena, and their name comes from the spread nature of the echoes that they produce on ionosondes [*Berkner and Wells*, 1934]. They can also be detected by coherent and incoherent scatter radars, in situ space probes, radio propagation and scintillation experiments, and airglow. For a comprehensive overview of these nighttime phenomena, the reader should consult *Hysell* [2000].

The Jicamarca radar which is sensitive to the 3-m plasma irregularities produced during ESF events, has contributed extensively to the understanding of these very common nighttime phenomena [e.g., *Hysell*, 2000 and references therein]. The daytime occurrence of these 3-m irregularities is very puzzling, not only because most observations are confined to the nighttime, but physically they are harder to explain considering the stabilizing effect of the E-region conductivity during the day. On the other hand, topside sounders have detected irregularities almost until noon [*Dyson*, 1977].

2. Interferometric and Dual-beam Observations

In Figure 1 we show the antenna setup and pointing directions used for these observations, which are used for the incoherent scatter east-west mode [*Kudeki et al.*, 1999]. Briefly, the Jicamarca antenna is configured to point simultaneously in two directions, using two independent systems pointing $\sim$2.5° to the east and west of the geomagnetic meridional plane, respectively. The thick oval represent the half power region of each beam which are labeled by the letters E and W, respectively. The independence of the systems is obtained using two orthogonal polarizations, one for each transmitting beam. Associated with each pointing direction is a two-antenna receiving interferometer consisting of rectangular sections of the same polarization as the one used in transmission, i.e., the rectangular sections NW (composed of the North and West quarters) and SE are used for the East beam; and the rectangular sections NE and SW are used for the West beam. The loci of perpendicularity to the magnetic field are shown for heights 400 (plus signs), 800 (stars) and 1200 km (diamonds) above Jicamarca, according to the IGRF2000 magnetic field model. It is important to note that both interferometer baselines are $\sim$45° from the magnetic field lines. More specific details on the experimental setup are presented by *Kudeki et al.* [1999].

The measurements were conducted with a 10 ms interpulse period (IPP) (1500 km), and 3-baud Barker coded transmitted pulses with a total width of 300 μs and a baud width of 100 μs to provide a nominal range resolution of 15 km with decoded returns. During normal incoherent scatter

[1]Also at Laboratorio de Física, Universidad de Piura, Piura, Perú

Paper number 2001GL013404.
0094-8276/01/2001GL013404$05.00

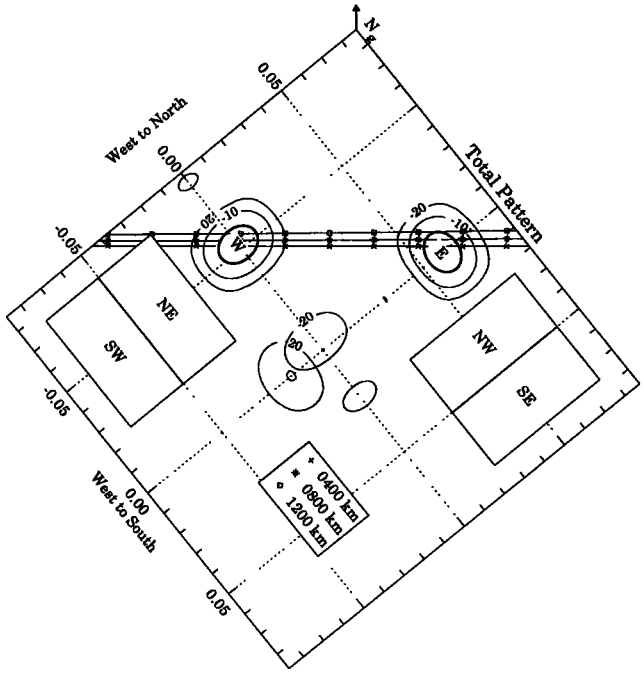

Figure 1. Antenna configuration. Two beams were transmitted, one pointing to the East (E) and one pointing to the West (W). A sketch of the receiving interferometer for each pointing direction is shown below/beside each beam. The loci of perpendicularity to the magnetic field are shown for 400, 800 and 1200 km above Jicamarca.

observations the sampling window is between 45 and 930 km. Complex raw data are recorded for each of the four receiving channels.

Having noticed the presence of echoes at higher altitudes, we changed to a higher sampling window, namely between 500 and 1400 km, during the time interval 1440 to 1530 LT. The first echoes were outside the original sampling window, so there are no digital records about when they started. Since the phenomenon is not common, we varied the IPP to exclude range aliasing from other sources (e.g., the Moon, ionospheric echoes from higher altitudes). The echoes remained in the same position in the oscilloscope, proving that the echoes were coming always from the topside of the F region.

In Figure 2 we show an example of the spectral characteristics of daytime ESF after coherent integration. As one can see, these irregularities are very strong and present relatively long correlation times (i.e., spectral widths more than two orders of magnitude narrower than incoherent scatter).

The top row of Figure 2 corresponds to the spectra (2a and 2b), power profiles (including noise) (2c), normalized cross spectral magnitude or coherence (2d), and cross spectral phase (2e) for the West data. Similar plots are shown for the East data in the bottom row. The cross spectra have been normalized with respect to signal power (no noise).

From the spectral data, we get values of Doppler shifts (v_d), spectral widths, and signal-to-noise ratio (SNR). The coherent echoes (above ~950 km) are much stronger in the West beam than in the East beam (~10 dB) and are up to two orders of magnitude stronger than the incoherent scatter echoes at the F peak. On the other hand, the incoherent scatter echoes show similar power profiles in both beams, giving us confidence on the good sensitivity of both systems. In both beams, $|v_d| < 1$ m s^{-1} and the spectral widths have comparable magnitudes.

In addition, there are significant differences in power (Figure 2h) between the two receiving antennas of the East beam (~5-10 dB), particularly above 950 km (thin profiles show lower values than the thick profiles). Note also that the power profile of the NW antenna (thick line) has a similar shape than the profiles of the West pointing antennas (i.e., SW and NE). Because of the similarity in the IS profiles (below 800 km) and some of the coherent profiles (between 850 and 950 km), we are also certain of the good sensitivity of both receiving antennas of the East beam. We discuss these differences in section 3.

The coherence values for the West data (i.e., SW, NE) are very high (>0.9), while those from the East data (i.e., NW, SE) are less than 0.5. The phase values are pretty much constant in frequency (only one gray tone) when the coherence is high.

For each beam we have only one interferometer baseline, which is not enough to determined the complete horizontal sizes and position of the irregularities. However, knowing that these irregularities are highly field-aligned, i.e., very aspect sensitive in the north-south (NS) direction, we can

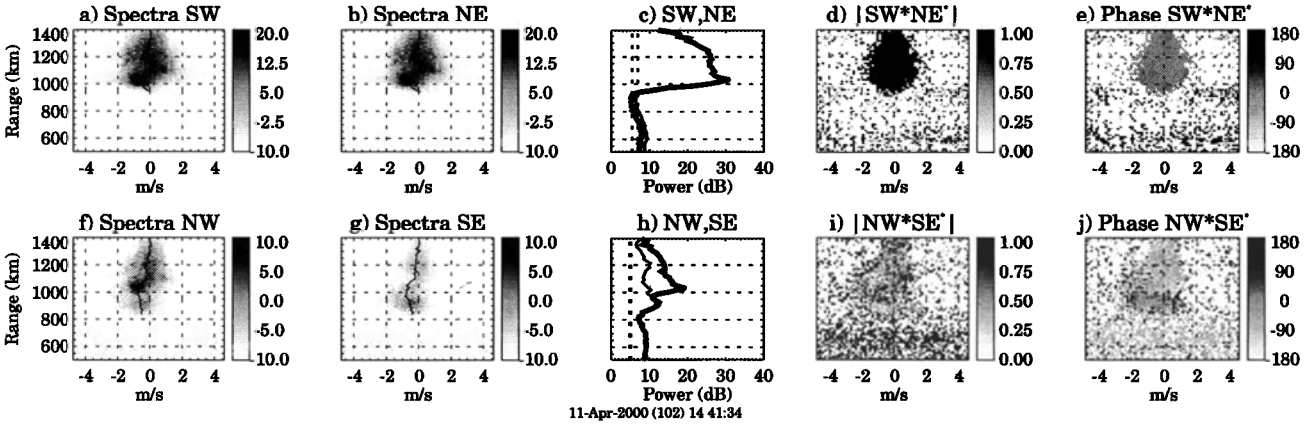

Figure 2. Spectrograms, power profiles and cross spectrograms (magnitude and phase) for the two interferometers, top row for the West beam data and bottom row for the East beam data.

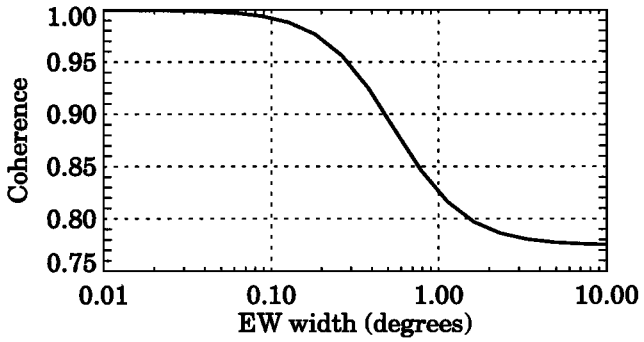

Figure 3. Calculated theoretical values for different EW angular widths of a single field-aligned anisotropic Gaussian blob.

infer the aspect sensitivity width (or Brightness width) in the east-west (EW) direction from the measured coherence values. We have used equations 6 and 7 of *Chau et al.* [2000] which apply for a general two dimensional approach, take into account the geometry of the experiment (antenna sizes and positions), and assume an anisotropic Gaussian blob centered on the beam and with its axes aligned parallel (NS) and transverse (EW) to the magnetic field lines. This approach is needed given that the interferometer baselines for both beams are not aligned with either the parallel or the transverse directions to the magnetic field. In Figure 3 we show the coherence values of the interferometer as a function of the EW angular width. Notice that when the EW width of the blob is larger than the resulting antenna beam width of the transmitting and receiving patterns, the coherence is mostly determined by the latter, and approaches the value of ~0.77.

In Figure 4 we show the range-time contours of (a) SNR, and (b) EW aspect sensitivity width (from coherence values). Figure 4c shows the time series of cross-correlation phases for different ranges with different gray tones for each range. The EW widths are as small as 0.2°, and there are times (e.g., around 1458 LT) when EW width approaches the antenna beam width. For most of the heights, the phase slope as function of time is very small ($\sim 0.006^\circ s^{-1}$) and corresponds to very small EW drift velocities of about 0.5 m s^{-1} westward.

We are not showing the results of the east beam, because the SNR was very weak and the coherence was low. Moreover, the East echoes started at lower ranges (850 km) and lasted for the same time as the west echoes (see section 3 below).

In general, the measured vertical drifts at *F*-region heights were ~15 m s^{-1} upward as usual, while the Doppler velocities of the irregularities (not shown here) were between -1 and 1 m s^{-1}. The *F*-region zonal drifts were ~30 m s^{-1} westward also close to usual values. As it was shown by *Fejer et al.* [1985], these drift values are not expected to vary much with altitude, particularly for this time of the day and for solar max conditions. The other ionospheric conditions before, during, and after the occurrence of these irregularities were also about normal for this time of the year, i.e., $K_p = 2$ (quiet conditions), $f_oF_2 = 13.50$ MHz and $F10.7 = 182.4$.

3. Discussion

As we discuss below, most of our observations, particularly those above 950 km, can be explained if we assume an anisotropic Gaussian blob with the following characteristic features: (1) infinitely elongated in the NS direction (i.e., field aligned), (2) variable width in the EW direction, and (3) centered off-vertical in the EW direction. These features could represent different physical mechanisms (e.g., a small blob with variable EW widths or a large aspect-sensitive blob, larger than the beam width) but given our current one-baseline configuration, it is difficult for us to get a definite description of the actual scattering mechanism. We will limit our discussion to the observations and the one-blob characteristic model.

The fact that we consider the irregularities to be field aligned is highly justified. From a physical point of view, ambipolar diffusion along the magnetic field would not allow the buildup of density fluctuations with long coherence time at any angle other than perpendicular to the magnetic field, especially at wavelengths much shorter than the ion mean free path such as the 3-m wavelength that concerns us here. Only at angles almost perpendicular to the magnetic field, the projected velocity of the gyro centers of the electrons are small enough to explain the small Doppler widths (large coherence time).

As we saw in section 2, the EW widths vary considerably with time and height and can be as low as 0.2°. Moreover, there is a clear correlation with the intensity of the echoes, i.e., the stronger the echoes the narrower the EW widths.

We are assuming that our characteristic blob is centered off-vertical, because the echoes are consistently stronger (more than 10 dB) in the West beam than in the East beam. Moreover, the echoes from the East receiving antennas are coming from almost the same volume as the echoes from the West antennas, given the very good agreement in the shape of the power profiles and the spectral information (not shown here), particularly from the echoes received at the NW antenna.

With our current interferometer, the angular ambiguity is less than 1.15°, so we are not able to use the phase in-

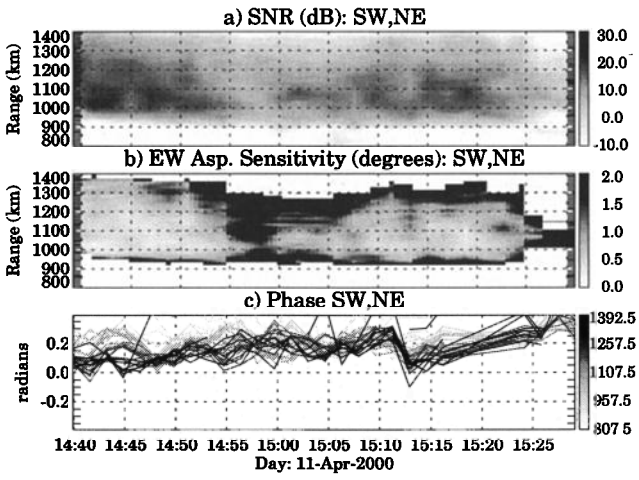

Figure 4. Range-time diagrams of (a) SNR, (b) aspect sensitivity width in the East-West direction, and (c) interferometer phase, using the West interferometer. Only data with SNR greater than -6 dB are shown.

formation to determine the absolute origin of the echoes. However, we have plotted the antenna patterns for both the East and West beams at the loci of perpendicularity for different heights (results not shown here), and we are certain that the echoes are coming around the main lobe of the West beam, i.e., the East antennas are seeing the echoes via sidelobes. Therefore, our characteristic blob is centered around 2.5° to the west of the geomagnetic meridional plane for all the altitudes (950-1450 km). In addition, from the phase information we can determine if the characteristic blob is drifting across the beam. From Figure 4c, we can see that there is a very small drifting, i.e., phase slope is very small for all ranges and therefore the westward drift ($\sim$0.5 m s^{-1}) is much smaller than the zonal drift measured at the lower heights. The small EW velocity will also explain why the blob did not drift from one beam (E) to the other (W).

So far, the observations we have discussed support our characteristic blob. However there are two observations that do not support our model (1) the difference in power between the two East pointing antennas (i.e., NW, SE) and the low coherence between their signals, and (2) the existence of lower echoes (850-950 km) in the East beam. The former observations can be explained by slight differences in the sidelobes of the two East pointing antennas, particularly in the region close to the antenna pattern nulls. Above, we mentioned that the East echoes were coming via sidelobes, but if the sidelobes are not the same, both antennas will receive echoes from slightly different volumes.

The lower echoes observed by the East beam could be explained by another localized blob, located at a lower altitude and centered at a different off-vertical position. However, since the coherence is lower than expected, we also think they are coming from slightly different sidelobes. This time the power profiles for the two East receiving antennas are similar, but the Doppler information is different (results not shown here).

4. Concluding Remarks

We have reported a new event of the very uncommon daytime F-region irregularities. The main characteristics of our observations are similar to those observed on previous events, namely that daytime spread-F-like irregularities (1) are up to two orders of magnitude stronger than incoherent scatter echoes, (2) occur between 1400 and 1600 LT, (3) present very small Doppler shifts, and (4) have long correlation times. On the other hand, the irregularities we have observed occur at higher altitudes ($\sim$950-1400 km) than those seen before ($\sim$600-1000 km).

In addition, from our observations, these echoes (1) are aspect sensitive in the east-west magnetic direction with widths as small as 0.2°, particularly when the echoes are strong, (2) they drift very slowly across the beam, and (3) are localized in the EW direction.

Although the daytime F region irregularities have some characteristics similar to those of nighttime ESF, i.e., enhanced power over the incoherent scatter echoes and longer correlation times, we are not in position to propose a definite physical explanation for their existence. For future observations, it would be important to know the ionospheric conditions at E-region heights corresponding to the same magnetic tubes, to get a better insight on the physical mechanism behind these echoes.

Acknowledgments. The authors gratefully acknowledge the dedication of Gerardo Vera to the Jicamarca operations. We thank Don Farley and Dave Hysell for their comments and suggestions during the early stages of the manuscript. The Jicamarca Radio Observatory is operated by the Geophysical Institute of Perú, with support from the NSF Cooperative Agreement ATM-9408441 and ATM-9911209. J.L.C. was partially supported by the NSF under agreement ATM-9813910.

References

Berkner, L. V., and H. W. Wells, F-region ionosphere investigation at low latitudes, *Terrestrial Magnetism*, *39*, 215, 1934.

Chau, J. L., R. J. Doviak, A. Muschinski, and C. L. Holloway, Tropospheric measurements of turbulence and characteristics of bragg scatterers using the Jicamarca VHF radar, *Radio Sci.*, *35*, 179–193, 2000.

Dyson, P. L., Topside irregularities in the equatorial ionosphere, *J. Atmos. Sol. Terr. Phys.*, *39*, 1269–1275, 1977.

Fejer, B. G., E. Kudeki, and D. T. Farley, Equatorial F region zonal plasma drifts, *J. Geophys. Res.*, *90*, 12,249–12,255, 1985.

Hysell, D. L., An overview and synthesis of plasma irregularities in equatorial spread F, *J. Atmos. Sol. Terr. Phys.*, *62*, 1037–1056, 2000.

Kudeki, E., S. Bhattacharyya, and R. F. Woodman, A new approach in incoherent scatter F region E x B drift measurements at Jicamarca, *J. Geophys. Res.*, *104*, 28,145–28,162, 1999.

Woodman, R. F., J. E. Pingree, and W. E. Swartz, Spread-F-like irregularities observed by the Jicamarca radar during the day-time, *J. Atmos. Sol. Terr. Phys.*, *47*, 867–874, 1985.

J. L. Chau and R. F. Woodman, Radio Observatorio de Jicamarca, Apartado 13-0207, Lima, Perú (e-mail: chau@geo.igp.gob.pe; ron@geo.igp.gob.pe)

(Received May 7, 2001; accepted July 5, 2001.)